

Structural and magnetic aspects of the metal insulator transition in $\text{Ca}_{2-x}\text{Sr}_x\text{RuO}_4$

O. Friedt,¹ M. Braden,^{1,2} G. André,¹ P. Adelman,² S. Nakatsuji,³ and Y. Maeno^{3,4}

¹*Laboratoire Léon Brillouin, C.E.A./C.N.R.S., F-91191-Gif-sur-Yvette CEDEX, France*

²*Forschungszentrum Karlsruhe, IFP, Postfach 3640, D-76021 Karlsruhe, Germany*

³*Department of Physics, Kyoto University, Kyoto 606-8502, Japan*

⁴*CREST, Japan Science and Technology Corporation, Kawaguchi, Saitama 332-0012, Japan*

The phase diagram of $\text{Ca}_{2-x}\text{Sr}_x\text{RuO}_4$ has been studied by neutron diffraction on powder and single-crystalline samples. The experiments reveal antiferromagnetic order and structural distortions characterized by tilts and rotations of the RuO_6 -octahedra. There is strong evidence that the structural details of the isostructural samples tune the magnetic as well as the electronic behavior. In particular we observe for low Sr-concentration a metal insulator transition associated with a structural change and magnetic ordering.

PACS numbers: 61.12.-q, 64.70.-p, 74.70.-b, 75.50.Ee

INTRODUCTION

Layered perovskite ruthenates have attracted considerable interest since the discovery of superconductivity in Sr_2RuO_4 , which remains till today the only known superconductor isostructural to the cuprates [1]. It is, therefore, expected that this material can give further insight into the mechanism of High Temperature Superconductivity. However, the origin of the spin-triplet pairing in Sr_2RuO_4 [2] is far from understood. There is reasonable evidence that in this material a coupling between electrons and magnetism is essential: for example magnetic susceptibility [3] and low temperature specific heat [4] exhibit similar enhancements. It has been suggested that ferromagnetic fluctuations are dominating the interaction leading to an unconventional pairing of p-wave symmetry [5]. This proposal was mainly inspired by the fact that the perovskite SrRuO_3 is indeed an itinerant ferromagnet [6]. The substitution of Sr by Ca in the layered compound yields rather different physical properties. First Ca_2RuO_4 is an insulator at low temperatures [7] and second it orders antiferromagnetically [8, 9], which clearly indicates that considering Sr_2RuO_4 as being close to ferromagnetic order is an oversimplification. More recently band structure analyses on Sr_2RuO_4 have predicted that the magnetic susceptibility presents dominating peaks at incommensurate wave vector positions, $q_0 = (2\pi/3a, 2\pi/3a, 0)$, which arise from Fermi-surface nesting [10]. Inelastic neutron scattering studies have perfectly confirmed these features [11]. In order to get an insight to the relation between these incommensurate peaks in the Sr_2RuO_4 susceptibility and the antiferromagnetic order in Ca_2RuO_4 it appears essential to study the entire phase diagram of $\text{Ca}_{2-x}\text{Sr}_x\text{RuO}_4$.

The physics of $\text{Ca}_{2-x}\text{Sr}_x\text{RuO}_4$ attracts interest not only in the context of the superconductivity in Sr_2RuO_4 . In our first paper we have demonstrated that in a Ca_2RuO_4 sample containing excess oxygen ($\text{Ca}_2\text{RuO}_{4.07}$, O- Ca_2RuO_4), one finds a structural transition from a metallic high-temperature phase into a non-metallic dis-

torted low-temperature phase hence a metal-insulator transition [8]. The observation of the antiferromagnetic order in the non-metallic phase suggests the interpretation that this transition is of the Mott-type. The high temperature metallic phase of O- Ca_2RuO_4 is characterized by an octahedron shape almost identical to that observed in Sr_2RuO_4 , whereas the in-plane Ru-O bond lengths are significantly enhanced in the low temperature insulating phase. In addition there is a stronger tilt of the RuO_6 octahedra in the low temperature phase. The structural transition is of the first order type, as seen in the large hysteresis with coexistence of the two phases, and presents a lattice expansion of $\frac{\Delta V}{V} \sim 1\%$ upon cooling. Recently Alexander et al. have found a sudden increase in the resistivity of stoichiometric Ca_2RuO_4 at 357 K [12], suggesting that the metal insulator transition seen in O- Ca_2RuO_4 occurs just at higher temperature in the stoichiometric compound. Nakatsuji et al. have revealed the entire magnetic phase diagram of $\text{Ca}_{2-x}\text{Sr}_x\text{RuO}_4$, and found the metal insulator transition by resistivity and magnetic susceptibility measurements [13, 14]. They observe that the anomalies in the resistivity are rapidly shifted to lower temperature for increasing Sr-content, for $x > 0.2$ samples stay metallic till low temperature. Also Cao et al. report a decrease of the metal insulator transition temperature upon Sr-doping; in addition they observe the similar suppression for La-doping [15]. However, no diffraction study on structural aspects of the metal insulator transition as function of doping has been reported so far.

In many aspects the metal insulator transition in $\text{Ca}_{2-x}\text{Sr}_x\text{RuO}_4$ resembles that in V_2O_3 [16, 17]; the simpler crystal structure in the case of the ruthenate should be favorable for the analyses and their understanding.

We have extended our previous diffraction studies to the entire Sr-content range in $\text{Ca}_{2-x}\text{Sr}_x\text{RuO}_4$ proving that the structural distortion accompanying the metal insulator transition persists to $x \sim 0.15$ in O-stoichiometric samples. For higher Sr-content we find a distinct crystal structure, space group $I4_1/acd$, which again presents

a structural phase transition upon cooling, however, between two metallic phases.

EXPERIMENTAL

The stoichiometric sample of Ca_2RuO_4 (S- Ca_2RuO_4) used already in our previous work has been further analyzed at higher temperatures. In addition we have prepared samples of $\text{Ca}_{2-x}\text{Sr}_x\text{RuO}_4$ with $x=0.1, 0.2, 0.5, 1.0$ and 1.5 by the technique described in Ref. [7], details will be given else-where [18]. Thermogravimetric studies indicate a stoichiometric oxygen content in these mixed compounds. All samples were characterized by x-ray diffraction and by magnetic measurements.

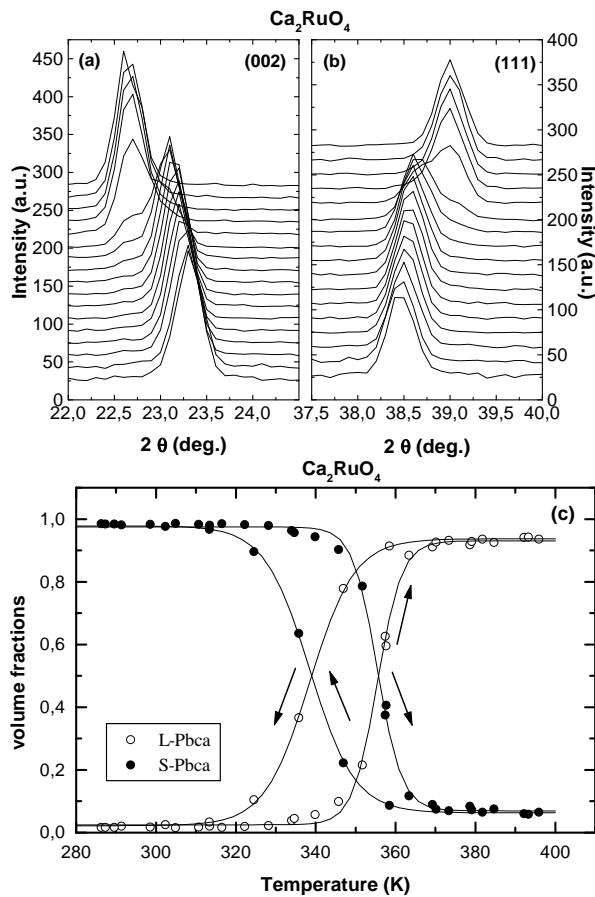


FIG. 1: Comparison of the high flux diffraction patterns, showing the (002) (a) and (111) (b) reflections, obtained in stoichiometric Ca_2RuO_4 at temperatures between 286 and 400 K. The lowest lines correspond to $T=286$ K and the following one approximately to 5 K steps. (c) Temperature dependence of the partial volume fractions of the L-Pbca and S-Pbca phases for Ca_2RuO_4 . The temperature variation is indicated by arrows.

Neutron diffraction studies were performed at the OR-PHEE reactor using the two diffractometers 3T.2 ($\lambda =$

1.226 Å) and G4.1 ($\lambda = 2.43$ Å). With the shorter wavelength instrument it is possible to perform complete Rietveld structure analyses whereas the longer wavelength multi-counter machine offers a high flux permitting the measurement of temperature dependencies. For more details of the diffraction analyses see our first paper [8].

Two single-crystals with $x=0.2$ and $x=0.5$ were obtained by a floating zone technique; these were examined on the two-axis diffractometer 3T.1 using pyrolytic graphite monochromator and filters.

RESULTS AND DISCUSSION

Metal insulator transition in S- Ca_2RuO_4 and in $\text{Ca}_{1.9}\text{Sr}_{0.1}\text{RuO}_4$

The strong temperature dependence of the structural parameters of S- Ca_2RuO_4 observed near room temperature indicates a structural phase transition in the temperature range 350–400 K. Indeed such a transition has been recently reported by Alexander et al. based on x-ray diffraction and resistivity studies [12]. In a first view, one might argue that the transition in O- Ca_2RuO_4 is just shifted to higher temperature in the stoichiometric sample, but the detailed structure analysis presents significant differences.

Using a cryo-furnace the structure was studied on G4.1 by recording a complete hysteresis cycle. At temperatures near 340 K, we already observe two phases, the low-temperature phase is characterized by a small c -lattice parameter (S-Pbca) compared to the high temperature phase with long c (L-Pbca); the averaged in-plane parameter exhibits the opposite behavior as can be seen in Fig. 1 (b). The transition in stoichiometric Ca_2RuO_4 is sharper than in O- Ca_2RuO_4 ; at 365 K it is almost complete, and at 395 K there is no sign of the low temperature S-Pbca phase in the high flux patterns, parts of the high flux patterns are shown in Fig. 1 (a),(b). To avoid possible variation in oxygen stoichiometry during the hysteresis cycle, the temperature was limited to 400 K. Also the high resolution pattern obtained at 400 K can be refined by a single S-Pbca-phase, the results are given in Table I. (Throughout the paper we use the same notations as in ref. [8]; O(1) denotes the oxygen in the RuO_2 -planes and O(2) the apical one. The rotation angle is unique and designed by Φ , whereas the tilt angle may be determined at the two oxygen sites, Θ -O(1) and Θ -O(2); in the notation used here the tilt is always around an axis close to the b -axis in Pbca.) In Fig. 1 (c) we show the temperature dependence of the L- and S-Pbca-phase volumes. The transition temperature obtained in up-strike, $T_S=356$ K, is in excellent agreement to that observed by Alexander et al. [12], $T_S=357$ K. The observed hysteresis of about 20 K clearly confirms the first order nature of the transition. We conclude that

the combined electronic and structural transition first observed in $\text{O-Ca}_2\text{RuO}_4$ also occurs in the stoichiometric compound.

In order to complete the study of the phase transition in stoichiometric Ca_2RuO_4 high resolution patterns have been recorded at 400 and at 180 K. The structure of the high-temperature L-Pbca-phase could not be established unambiguously in $\text{O-Ca}_2\text{RuO}_4$ [8]. Space group Pbca combines a rotation of the octahedra around the c -axis with a tilt around an axis parallel to an edge of the octahedron basal plane. In contrast in space group $\text{P2}_1/\text{c}$ the tilt can be about an arbitrary direction, in particular around a RuO-bond. The difference in the two symmetries may be easily tested in the O(1)-positions, the tilt around the Ru-O-bond displaces only one O(1)-site parallel to c , whereas the tilt around an axis parallel to the edge displaces all O(1)-positions about the same distance. In other words, in Pbca all O(1)-sites are equivalent whereas there are two of them in $\text{P2}_1/\text{c}$. In the cuprates the two tilt schemes correspond to the LTO and LTT phases, see for example [19]. In the excess oxygen compound a better description of the data was obtained in space group $\text{P2}_1/\text{c}$ and in particular free refinement of the two distinct O(1)-displacements along c led to significant difference with one displacement almost vanishing, leading to a LTT equivalent tilt-scheme. The structure was finally refined with one O(1)-site being fixed at $z=0$. In case of the stoichiometric compound at 400 K this is definitely not an appropriate model. In space group Pbca one obtains a R-value of 5.39% which increases to 5.62% for the $\text{P2}_1/\text{c}$ -model with one $z\text{-O}(1)$ fixed to zero. Refining the $\text{P2}_1/\text{c}$ phase independently still gives a lower R-value than Pbca, but this difference is not significant any more. Therefore we conclude that the high temperature structure in stoichiometric Ca_2RuO_4 has the same space group Pbca as the low temperature structure. We differentiate these phases as L-Pbca and S-Pbca respectively due to their different c -parameters. The large amount of excess oxygen ($\delta=0.07$ in $\text{Ca}_2\text{RuO}_{4+\delta}$) seems to be responsible for the distinct diffraction pattern in the excess O compound.

Combining the new and the previous results [8] we get the entire picture of the phase transition in S- Ca_2RuO_4 . Fig. 2 presents the Ru-O bond-lengths, which show a discontinuous change at the L-Pbca-S-Pbca transition: the in-plane bonds become elongated and the out-of-plane one is shrinking upon cooling. Close to the transition – but in the S-Pbca phase –, the octahedron is still elongated along c in the temperature range 300–330 K. Upon further cooling one observes a continuous and even larger change in the same sense: the octahedron at low temperature is finally flattened along c . The edge lengths of the octahedron basal plane also show a discontinuous effect at the transition followed by a pronounced change in the S-Pbca phase. In accordance to the elongation of the Ru-O(1)-bonds these lengths increase upon cooling into the

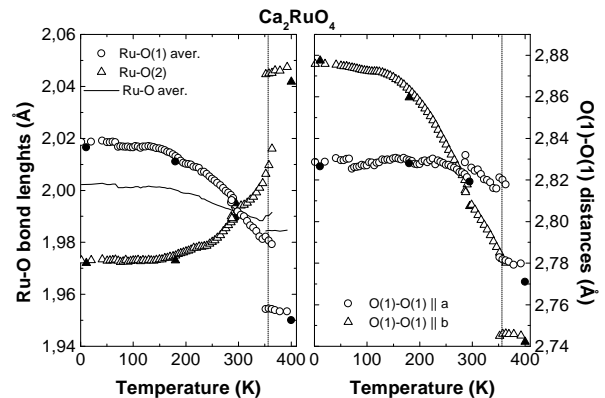


FIG. 2: Temperature dependence of the RuO(1)-bond distances in stoichiometric Ca_2RuO_4 and that of the edge lengths of the octahedron basal plane.

S-Pbca-phase where they are still split, the octahedron basal plane is shorter along the tilt axis immediately below the transition. Upon further cooling, the ratio, however, becomes inversed, and the basal plane is strongly stretched along the tilt axis.

In La_2CuO_4 [19] and also in all L-Pbca phase ruthenates studied here, the orthorhombic splitting is opposite to the expectation of a rigid tilt, i.e. the lattice is longer perpendicular to the tilt-axis. This effect originates from the forces in the La-O- or Sr-O-layer where one distance strongly decreases due to the opposite displacements of an apical oxygen and a neighboring La/Sr-site. The stretching of the lattice perpendicular to the tilt axis reduces the pronounced shrinking of this bond and may be seen in the orthorhombic splitting. One should hence consider this behavior as the normal one arising from the structural arrangement. Nevertheless the elongation of octahedron basal plane might influence the electronic and magnetic properties, see the discussion below. The orthorhombic lattice in Ca_2RuO_4 is elongated along the tilt-axis at low temperature much more than what might be expected for a rigid octahedron tilt; the lattice constants are given in Fig. 3. It is the stretching of the octahedra which causes this orthorhombic splitting, and this behavior should be considered as highly anomalous.

The transition from L-Pbca to S-Pbca is further characterized by an increase in the tilt angles, $\Theta\text{-O}(1)(\Theta\text{-O}(2))$ increase from 7.5° (5.9°) at 400 K to 11.2° (9.2°) at 295 K. Upon cooling in the S-Pbca phase these angles first continue to increase till about 180 K and are almost constant below, see Fig. 6 in ref. [8]. The rotation angle decreases by about one degree during the transition into the S-Pbca phase and is constant over the whole S-Pbca temperature range.

In $\text{Ca}_{1.9}\text{Sr}_{0.1}\text{RuO}_4$ we find a structural transition similar to that observed in Ca_2RuO_4 . Fig. 4 presents the volume fractions of the L-Pbca and S-Pbca phases as a

Composition	x=0.0	x=0.0	x=0.1	x=0.1	x=0.2	x=0.2	x=0.5	x=0.5
Temperature	180 K	400 K	10 K	300 K	10 K	300 K	10 K	300 K
Space group	<i>S-Pbca</i>	<i>L-Pbca</i>	<i>S-Pbca</i>	<i>L-Pbca</i>	<i>L-Pbca</i>	<i>L-Pbca</i>	<i>I4₁/acd</i>	<i>I4₁/acd</i>
<i>a</i> (Å)	5.3945(2)	5.3606(3)	5.4207(4)	5.3494(3)	5.3304(4)	5.3295(5)	5.3195(1)	5.3395(1)
<i>b</i> (Å)	5.5999(3)	5.3507(3)	5.4802(6)	5.3420(3)	5.3190(5)	5.3232(4)	“	“
<i>c</i> (Å)	11.7653(5)	12.2637(4)	11.9395(6)	12.3219(4)	12.4094(7)	12.4506(7)	2 · 12.5867(3)	2 · 12.5749(3)
Vol (Å ³)	355.41(3)	351.76(2)	354.67(5)	352.12(3)	351.84(5)	353.22(5)	2 · 356.17(1)	2 · 358.51(1)
ϵ	0.0187	0.0009	0.0055	0.0007	0.0011	0.0006	/	/
<i>R_{wp}</i> (%)	5.81	5.39	5.16	5.84	5.95	5.48	5.15	4.26
Ca <i>x</i>	0.0042(4)	0.0110(5)	0.0083(4)	0.0099(6)	0.0133(7)	0.0103(15)	0	0
<i>y</i>	0.0559(4)	0.0269(5)	0.0425(4)	0.0214(6)	0.0169(9)	0.0157(12)	1/4	1/4
<i>z</i>	0.3524(2)	0.3479(1)	0.3505(2)	0.3481(1)	0.3475(2)	0.3482(2)	0.5492(1)	0.5494(1)
<i>U_{iso}</i> (Å ²)	0.0052(5)	0.0112(4)	0.0039(5)	0.0053(6)	0.0073(4)	0.0138(9)	0.0022(3)	0.0090(3)
Ru <i>U_{iso}</i> (Å ²)	0.0025(4)	0.0050(4)	0.0011(3)	0.0045(4)	0.0007(4)	0.0029(5)	0.0014(3)	0.0042(3)
O(1) <i>x</i>	0.1961(3)	0.1939(4)	0.1974(3)	0.1934(4)	0.1958(6)	0.1944(6)	0.1933(2)	0.1949(2)
<i>y</i>	0.3018(4)	0.3064(4)	0.3016(3)	0.3056(4)	0.3064(6)	0.3070(6)	<i>x</i> + 1/4	<i>x</i> + 1/4
<i>z</i>	0.0264(2)	0.0147(2)	0.0229(1)	0.0127(2)	0.0126(3)	0.0075(6)	1/8	1/8
<i>U_{⊥-plane}</i> (Å ²)	0.0047(5)	0.0116(6)	0.0024(6)	0.0100(5)	0.0023(9)	0.0088(8)	0.0052(16)	0.0092(16)
<i>U_{∥-plane}</i> (Å ²)	0.0055(5)	0.0033(5)	0.0031(6)	0.0020(6)	0.0005(2)	0.0054(5)	0.0024(8)	0.0040(7)
<i>U_{long-axis}</i> (Å ²)	0.0112(10)	0.0205(8)	0.0171(9)	0.0245(12)	0.0166(16)	0.0228(18)	0.0152(6)	0.0211(6)
O(2) <i>x</i>	−0.0673(3)	−0.0386(3)	−0.0583(2)	−0.0340(4)	−0.0368(5)	−0.0187(14)	0	0
<i>y</i>	−0.0218(4)	−0.0067(4)	−0.0141(4)	−0.0079(6)	−0.0078(5)	−0.0051(10)	1/4	1/4
<i>z</i>	0.1645(2)	0.1656(1)	0.1645(1)	0.1649(1)	0.1652(2)	0.1644(2)	0.4568(1)	0.4568(1)
<i>U_⊥</i> (Å ²)	0.0093(5)	0.0169(6)	0.0070(5)	0.0151(5)	0.0044(7)	0.0162(10)	0.0084(3)	0.0142(3)
<i>U_∥</i> (Å ²)	0.0042(8)	0.0117(8)	0.0053(9)	0.0079(7)	0.0035	0.0051(10)	0.0050(7)	0.0080(7)
Ru-O(1) (Å)	2.004(2)	1.949(2)	1.987(2)	1.939(2)	1.927(3)	1.928(4)	1.929(1)	1.933(1)
	2.018(2)	1.950(2)	1.988(2)	1.948(2)	1.942(3)	1.937(3)	/	/
Ru-O(2) (Å)	1.973(1)	2.042(1)	1.991(2)	2.040(2)	2.060(3)	2.050(3)	2.059(3)	2.057(3)
Ru-O _{aver} (Å)	1.998	1.980	1.989	1.973	1.976	1.972	1.972	1.974
O(1)-O(1) a (Å)	2.828(1)	2.771(1)	2.822(1)	2.758(1)	2.750(2)	2.739(2)	2.727(2)	2.734(2)
O(1)-O(1) b (Å)	2.860(1)	2.742(1)	2.799(1)	2.739(1)	2.722(1)	2.727(2)	“	“
Vol RuO ₆ (Å ³)	10.64	10.34	10.48	10.27	10.28	10.21	10.21	10.25
Θ-O(1) (deg)	12.69(10)	7.49(10)	11.16(5)	6.52(10)	6.6(2)	3.9(3)	/	/
Θ-O(2) (deg)	11.19(8)	5.91(7)	9.40(7)	5.25(11)	5.59(10)	2.9(3)	/	/
Φ (deg)	11.93(5)	12.77(6)	11.77(5)	12.65(6)	12.47(9)	12.69(10)	12.78(3)	12.43(3)

TABLE I: Results of the high resolution powder diffraction analyses on Ca_{2-x}Sr_xRuO₄ at 300 and at 10 K. O(1) denotes the oxygen in the RuO₂-planes and O(2) the apical one. The rotation angle is unique and designed by Φ whereas the tilt angle may be determined at the two oxygen sites, Θ-O(1) and Θ-O(2). Note that in Pbca the tilt is always around the b-axis, whereas the orthorhombic splitting may change sign. *U_∥* and *U_⊥* denote the mean-square atomic displacements parallel and perpendicular to the Ru-O bonds. O(1)-O(1)||a,b denote the length of the edge of the octahedron basal plane along a,b respectively. Errors are given in parentheses and result from the least square fitting; therefore they do not take account of systematic errors and underestimate effects of correlations.

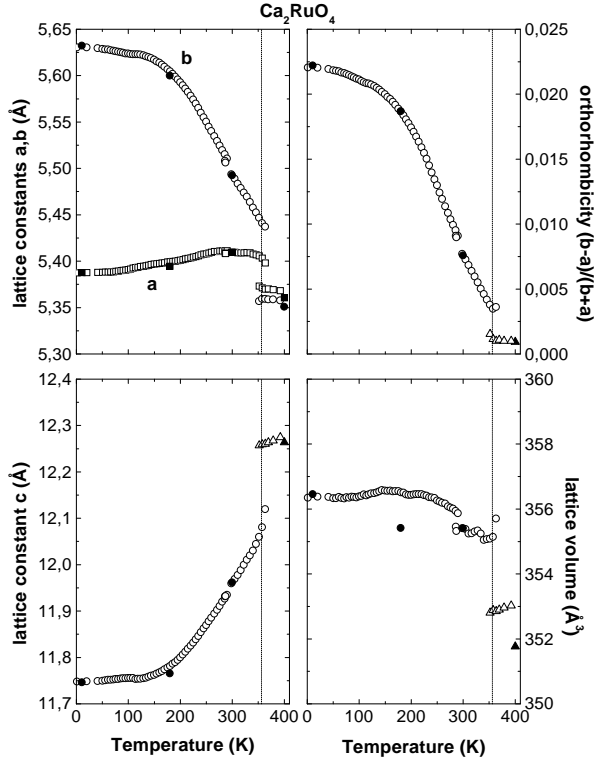


FIG. 3: Temperature dependence of the lattice parameters in stoichiometric Ca_2RuO_4 . Open symbol designate the results obtained from the high-flux patterns and closed symbols those from the high resolution studies.

function of temperature. The inset presents the hysteresis of the transition which amounts to about 50 K. For the discussion of any temperature dependent property one has to take account of this hysteresis.

The high resolution room temperature data in the metallic L-Pbca phase is again difficult to analyze. Refinements in space group Pbca and in space group $\text{P2}_1/\text{c}$ with or without fixed O(1)-site are very close concerning their R-values. However, like in S- Ca_2RuO_4 – and in contrast to O- Ca_2RuO_4 – the $\text{P2}_1/\text{c}$ fit does not suggest different O(1)- z -displacements. Powder diffraction alone, however, is unable to differentiate between Pbca and $\text{P2}_1/\text{c}$ space groups. A single crystal diffraction experiment on a single crystal of almost identical composition, $\text{Ca}_{1.85}\text{Sr}_{0.15}\text{RuO}_4$, definitely excludes the tilt around the RuO-bond [20]. Since $\text{P2}_1/\text{c}$ is a sub-group of Pbca, the description of Bragg reflection data must be better due to the larger number of free parameters. However an extremely small improvement of the R-value, 5.065% for the $\text{P2}_1/\text{c}$ -model compared to 5.078 % for the Pbca-model, does not support the symmetry reduction [20]. Therefore, we feel confident to analyze the powder diffraction patterns on excess oxygen free samples in the L-Pbca-structure.

The transition in $\text{Ca}_{1.9}\text{Sr}_{0.1}\text{RuO}_4$ is much better de-

fined than that in O- Ca_2RuO_4 and there is no L-Pbca phase remaining at low temperature. Therefore, it has been possible to analyze the structural details in this compound with the G4.1 data. Again high resolution patterns have been recorded at 295 and at 11 K with the results of the refinements given in Table I; high flux patterns were measured in temperature steps of 5 K upon heating. Fig. 5 presents the temperature dependence of the lattice parameters showing similar discontinuities at the transition, $T_S \simeq 175$ K upon heating, as the stoichiometric sample.

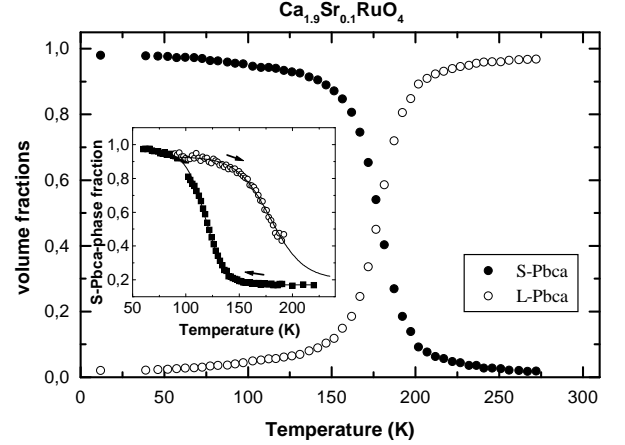


FIG. 4: Temperature dependence of the volume fractions of the L-Pbca and S-Pbca phases in $\text{Ca}_{1.9}\text{Sr}_{0.1}\text{RuO}_4$ measured on the high flux neutron diffractometer. The inset shows the hysteresis of the transition as obtained by x-ray diffraction.

In contrast to the stoichiometric compound, the temperature dependence of the structural parameters within the S-Pbca phase is only small. In analogy to Fig. 2, Fig. 6 presents the temperature dependent shape of the octahedra in $\text{Ca}_{1.9}\text{Sr}_{0.1}\text{RuO}_4$ (the slight deviations between the high resolution and high flux results must be attributed to the insufficient extent in Q -space of the latter data combined with the smaller orthorhombic splitting; nevertheless there is no doubt that these results show the correct tendencies). In $\text{Ca}_{1.9}\text{Sr}_{0.1}\text{RuO}_4$ too we find the discontinuous change at T_S : an increase in the in-plane bond lengths and a shrinking of the Ru-O(2)-distance. But in contrast to the stoichiometric compound the octahedron remains slightly elongated along c till the lowest temperatures. Also the octahedron edges parallel to the a, b -plane present the same discontinuous changes as S- Ca_2RuO_4 but not the continuous stretching along b in the Pbca phase. In particular, the octahedron remains elongated along the a -axis, i.e. perpendicular to the tilt axis. Due to the larger tilt this elongation may no longer over-compensate the lattice shrinking in the a -direction, the orthorhombic lattice is therefore longer along b .

In $\text{Ca}_{1.9}\text{Sr}_{0.1}\text{RuO}_4$ we also find the jump of the tilt

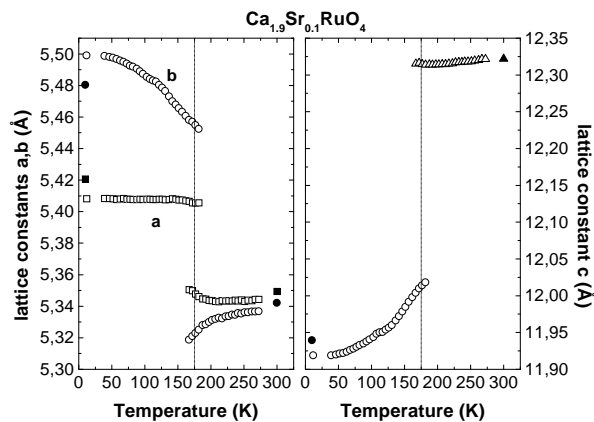


FIG. 5: Temperature dependence of the lattice parameters in $\text{Ca}_{1.9}\text{Sr}_{0.1}\text{RuO}_4$; open symbols designate the results obtained from the high flux studies and closed symbols those from the high resolution experiments.

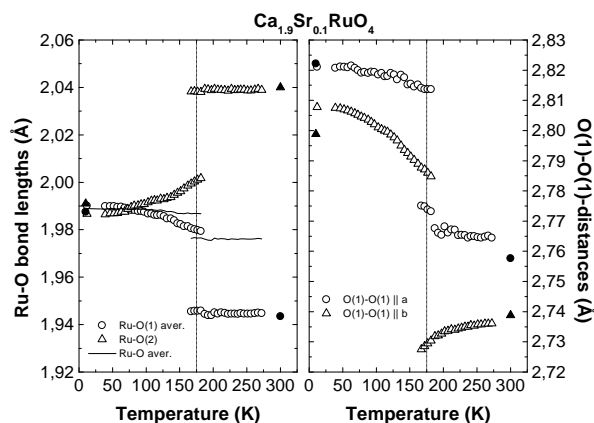


FIG. 6: Temperature dependence of the Ru-O bond distances and that of the octahedron basal-plane-edge lengths in $\text{Ca}_{1.9}\text{Sr}_{0.1}\text{RuO}_4$.

angles at T_S which remain almost constant in the Pbca phase. The transition in $\text{Ca}_{1.9}\text{Sr}_{0.1}\text{RuO}_4$ may be characterized as being identical to the one in the pure compound. However, as there are only minor changes of the structural parameters for $\text{Ca}_{1.9}\text{Sr}_{0.1}\text{RuO}_4$ below the phase transition, one may resume that the structure observed in the pure compound slightly below the transition, is stable to the lowest temperatures for the Sr-concentration $x=0.1$; positional and lattice parameters of S- Ca_2RuO_4 at 295 K and $\text{Ca}_{1.9}\text{Sr}_{0.1}\text{RuO}_4$ at 10 K are almost identical, see Table I and ref. [8].

$\text{Ca}_{1.9}\text{Sr}_{0.1}\text{RuO}_4$ also exhibits antiferromagnetic order below $T_N=143$ K, see Fig. 7. There is only one magnetic transition observed in neutron diffraction, and the magnetic arrangement is the B-centered one of La_2NiO_4 -type similar to the observation in O- Ca_2RuO_4 [8]. One may note that the direction of the ordered moment in

$\text{Ca}_{1.9}\text{Sr}_{0.1}\text{RuO}_4$ remains the b-axis, though the shape of the octahedron is different to that of the pure compound. The tilt-direction seems hence to be the element determining the spin-direction and not the stretching of the octahedron, which underlines the importance of anti-symmetric coupling parameters.

In Fig. 7 we compare the ordered magnetic moment and the magnetic susceptibility

That the antiferromagnetic transition manifests itself in the susceptibility is not astonishing and arises from the Dzyaloshinski-Moriya interaction. Weak ferromagnetism is much stronger in the ruthenates than in the cuprates due to the stronger spin-orbit coupling. The low temperature susceptibility in $\text{Ca}_{1.9}\text{Sr}_{0.1}\text{RuO}_4$ is even higher than the values reported for La-substituted Ca_2RuO_4 [15], therefore, one may assume that magnetic order in these samples too is mainly antiferromagnetic in nature. Nakatsuji et al. have observed also the electronic transition associated with an upturn in the resistivity in a series of samples of $\text{Ca}_{2-x}\text{Sr}_x\text{RuO}_4$ in the Sr-concentration range up to $x=0.2$ [13]. These observations show that the structural transition triggers the magnetic order and the insulating behavior, however the details of the coupling between structural magnetic and electronic transition for the highly Sr-doped samples need further clarification. The analysis of the existing data obtained in a cooling cycle is hampered by the fact that the down-stroke structural transition is below the intrinsic T_N in the S-Pbca phase; single crystals, however, shutter at the transition and therefore resistivity measurements upon heating become difficult to interpret.

Structure of $\text{Ca}_{2-x}\text{Sr}_x\text{RuO}_4$ with $x=0.2, 0.5$ and $x=1.0$

Upon further increase of the Sr-concentration the metal-insulator transition is suppressed slightly above $x=0.15$ [13]. The powder-sample of $\text{Ca}_{1.8}\text{Sr}_{0.2}\text{RuO}_4$ studied here does not exhibit the anomalous resistivity increase, nor does the one with $x=0.5$.

The high resolution powder patterns on $\text{Ca}_{1.8}\text{Sr}_{0.2}\text{RuO}_4$ indicate a mixture of the L-Pbca phase with a second phase whose space group was identified as being $I4_1/acd$. Also the sample with still higher Sr-content, $\text{Ca}_{1.5}\text{Sr}_{0.5}\text{RuO}_4$, was found in this symmetry. In space group $I4_1/acd$ the octahedra are rotated around the c-axis, however, with a stacking different to that in Pbca; in addition the tilt of the octahedra is not allowed. In $I4_1/acd$ the RuO_2 -planes separated by 12.5Å are distorted with an opposite phase which yields a doubling of the c-parameter. This symmetry is well known from related compounds like Sr_2IrO_4 [21, 22] or Sr_2RhO_4 [23]. The observation of a phase with only a rotational distortion agrees furthermore to the analysis of the phonon dispersion in Sr_2RuO_4 : it was reported that

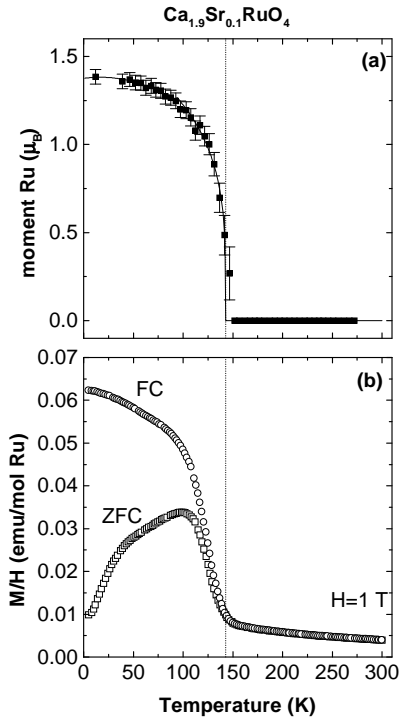


FIG. 7: (a) Temperature dependence of ordered magnetic moment obtained by refinement of the B-centered antiferromagnetic structure of La_2NiO_4 -type in $\text{Ca}_{1.9}\text{Sr}_{0.1}\text{RuO}_4$; (b) temperature dependence of the field-cooled and zero-field-cooled susceptibility measured on a part of the sample. All dependences were recorded upon heating.

only the rotational mode is close to instability [24]. By neutron diffraction the $I4_1/\text{acd}$ and Pbca phases may be easily distinguished, since the superstructure reflections related to the rotation occur at different l -values due to the distinct stacking, see for example the positions of the $(2\ 1\ 1)$ -reflections shown in Fig. 8.

As can be deduced from the doubled c -parameter in the $I4_1/\text{acd}$ phase, a continuous transition between these phases is not symmetry-allowed. The volume fraction of the $I4_1/\text{acd}$ phase in $\text{Ca}_{1.8}\text{Sr}_{0.2}\text{RuO}_4$ is small and upon cooling it decreases from 21% at room temperature to 12% at 11 K. The insertion of the smaller Ca enhances the internal mismatch which drives rotational as well as any tilt transition upon cooling. Therefore one may understand that the Pbca phase becomes more stable at low temperature. The Pbca phase in $\text{Ca}_{1.8}\text{Sr}_{0.2}\text{RuO}_4$ presents pronounced structural changes upon cooling. It is found that the free tilt in the Pbca -symmetry increases with a slight reduction of the rotation. Also this behavior seems to be the natural consequence of the higher Ca concentration.

A single crystal of composition $x=0.2$ showed a different behavior: a single phase $I4_1/\text{acd}$ structure at room temperature followed by a tilt transition upon cooling.

Since the transition between $I4_1/\text{acd}$ and Pbca is of first order, it appears likely that the structure of samples close to the phase boundary depends on their real structure. On the 3T.1-diffractometer the intensities of different reflections were followed as function of temperature for the single crystal of $\text{Ca}_{1.8}\text{Sr}_{0.2}\text{RuO}_4$. At low temperature several reflections – for example $(3\ 0\ 4)$ in $I4_1/\text{acd}$ notation – appear which are forbidden in the $I4_1/\text{acd}$ symmetry. The transition is continuous with only a minor first order contribution close to the transition. The type of the observed superstructure reflections clearly indicates that the low temperature phase possesses a non-vanishing tilt. However, the detailed analysis of this structure has to be performed by neutron diffraction on a four-circle diffractometer. Interestingly the tilt-distortion exhibits a different period along the c -axis, i.e. just one c -parameter ($c \sim 12\text{ \AA}$) whereas the period of the rotation is $2c$. In general the tilt-phonon-modes show a finite dispersion fixing the stacking sequence, due to the displacements of the apical oxygens [24]. The interaction of the two order-parameters corresponding to different propagation vectors, $q_1 = (0.5, 0.5, 0)$ and $q_2 = (0.5, 0.5, 0.5)$, might be an interesting problem; it certainly explains the first order phase transition occurring near $x=0.2$ as a function of Sr-content. The stronger tilt near $x=0.2$ forces the rotational distortion, whose stacking sequence is much less defined [24], into the same one- c -period. For the following we conclude that for a Sr concentration close to $x=0.2$, the structure needs a tilt distortion either in a sub-group of $I4_1/\text{acd}$ (single crystal) or in Pbca (powder). The tilt distortion causes an elongation of the octahedron basal plane, as can be seen in Table I and as it discussed above. Although the tilt may explain this elongation in a purely structural way, the elongation should influence the electronic band structure since the degeneration of the d_{xz} - and d_{yz} -bands is lifted, see below.

The high resolution patterns obtained on $\text{Ca}_{1.5}\text{Sr}_{0.5}\text{RuO}_4$ clearly indicate an unique $I4_1/\text{acd}$ phase. There is only little temperature dependence in the structure of $\text{Ca}_{1.5}\text{Sr}_{0.5}\text{RuO}_4$ as it is shown in Table I. In the $I4_1/\text{acd}$ -structure, there are only three positional parameters, $z\text{-Ca}$, $z\text{-O}(2)$ and $x\text{-O}(1)$ and only the latter changes significantly related to the increase of the octahedron rotation angle by about 3% between 295 and 11 K, from $12.43(3)^\circ$ to $12.78(3)^\circ$. In the high flux patterns, no indication for long range magnetic order has been observed yielding an upper boundary for a long range ordered magnetic moment of $0.15\mu_B$.

A small single crystal of $\text{Ca}_{1.5}\text{Sr}_{0.5}\text{RuO}_4$ has been studied on the 3T.1 thermal neutron diffractometer as function of temperature. The temperature dependence of the superstructure intensity shown in Fig. 9, indicates a second order phase transition similar to the one observed for $x=0.2$. The smaller Ca-content causes a reduced transition temperature and a weaker tilt at low temperature, as can be deduced from the smaller relative intensity ob-

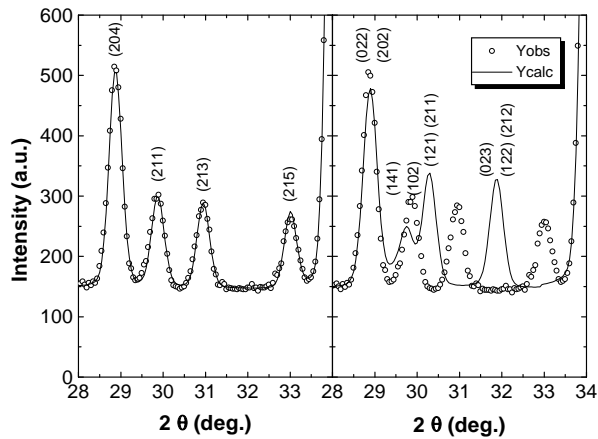


FIG. 8: Comparison of the powder diffraction patterns calculated for the rotational distortion in space group $I4_1/acd$ ($c \sim 24$ Å; left) and in space group $Pbca$ ($c \sim 12$ Å; right). The calculated patterns are compared to high resolution data observed for $Ca_{1.5}Sr_{0.5}RuO_4$.

served in this crystal, see Fig. 9. In the powder sample of the same composition, $x=0.5$, we find only a weak anomaly in the c -axis parameter, observed at 65 K. The c -parameter should be quite sensitive to an octahedron tilt, since the projection of the octahedra along c varies with the cosine of the tilt angle. As may be seen in Fig. 9, the superstructure reflections observed on the single crystal are not strong enough to be detected by powder neutron diffraction.

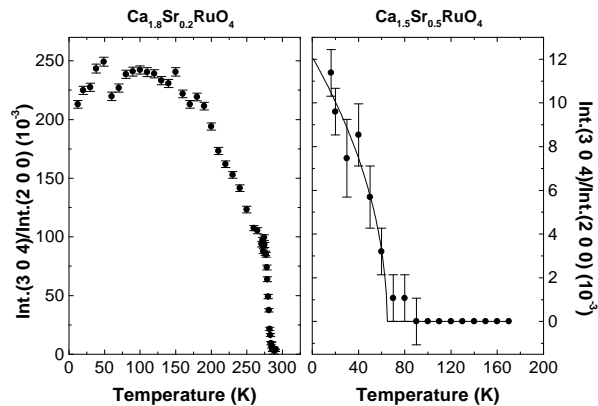


FIG. 9: Temperature dependence of (3 0 4) ($I4_1/acd$ notation) superstructure reflection intensity scaled to that of the (200) fundamental reflection in two single crystals of compositions $Ca_{1.8}Sr_{0.2}RuO_4$ (left) and $Ca_{1.5}Sr_{0.5}RuO_4$ (right).

The compound with $x=1.0$ was studied at room temperature and at 11 K by high resolution diffraction. We find at both temperatures a pure $I4_1/acd$ phase, however, there is evidence for disorder in the rotation scheme. The refinement was significantly improved by splitting the $O(1)$ -position into two sets of positions $(x, |x| + \frac{1}{4}, \frac{1}{8})$,

with $x=\pm\delta$ similar to the observation in [22] for Sr_2IrO_4 . The average rotation angle is temperature independent, $10.80(3)^\circ$ at room temperature and $10.75(3)^\circ$ at low temperature. Assuming that the square of the rotation angle varies linearly with the concentration, one would estimate the critical concentration for the appearance of the pure rotation distortion near $x=2.5$. From this consideration one would expect pure Sr_2RuO_4 to exhibit the same rotation in obvious contradiction to the observation that it remains undistorted till low temperature [25]. For a Sr concentration of $x=1.5$ we already do not find any long range rotation distortion order in the powder sample. However, there is sizeable diffuse scattering – strong enough to be detected by powder diffraction – indicating that the rotation distortion still exists on a short range scale. The single crystal diffraction studies on the pure Sr_2RuO_4 [25], which are more sensitive to diffuse scattering than powder diffraction, did not reveal any indication for a local rotational distortion. It seems interesting to study whether the existence of the local rotational disorder may be related to the worse metallic properties of the Ca-doped samples.

Phase diagram of $Ca_{2-x}Sr_xRuO_4$

According to the studies presented above the structural and magnetic phase diagram of $Ca_{2-x}Sr_xRuO_4$ is rather complicated, a schematic picture is given in Fig. 10, which also presents the results of the magnetic studies by S. Nakatsuji et al. [13]. In addition the tilt and rotation angles together with the deformation of the octahedron basal plane are depicted. At low temperature and for decreasing Sr-concentration, one passes from the undistorted K_2NiF_4 structure in pure Sr_2RuO_4 , space group $I4/mmm$, to a simple rotation $I4_1/acd$ in agreement to the low lying rotation mode in the pure compound [24]. An estimated boundary is included in the diagram in Fig. 10, though the transition is found to exhibit order-disorder character. For a Sr-concentration of $x=1.5$ only diffuse scattering representative of a short range rotational distortion is present. For $x=1.0$ the rotational angle already amounts to 10.8° ; the rapid suppression of the structural distortion in Sr-rich samples appears to be extraordinary it might hide some further effect. For much smaller Sr-content, near $x=0.5$, a combination of rotation and small tilt is found. This is realized either in a subgroup of $I4_1/acd$ or in $Pbca$. Further decrease of the Sr-content leads finally to the combination of the rotation and the large tilt in the $S-Pbca$ phase. The Sr-dependence of the tilt and rotation angles is resumed in Fig. 11. Most interestingly all these structural transitions are closely coupled to the physical properties.

The purely rotational distortion should be related to the c -axis resistivity since it modifies the overlap of the O -orbitals in c -direction. This rotation phase becomes

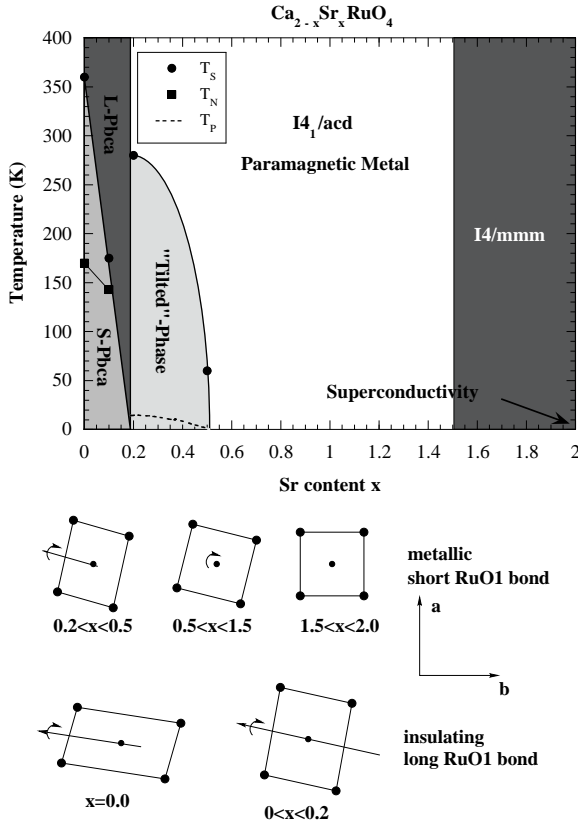


FIG. 10: Phase diagram of $\text{Ca}_{2-x}\text{Sr}_x\text{RuO}_4$ including the different structural and magnetic phases and the occurrence of the maxima in the magnetic susceptibility [13]. In the lower part, we schematically show the tilt and rotation distortion of the octahedra (only the basal square consisting of the Ru (small points) and the O(1) (larger points) is drawn) together with the elongation of the basal planes.

unstable against the tilt for Sr concentrations lower than 0.5, since in the single crystal with $x=0.5$ only a minor distortion has been observed, which remained undetectable in the powder sample. For the Sr-concentration of $x=0.2$ we already find tilt angles of about 7° at low temperature by powder neutron diffraction. Near $x=0.5$ there is hence the quantum critical point of the continuous tilt transition which coincides with a maximum in the low temperature magnetic susceptibility. For $x=0.5$, Nakatsuji et al. report a low temperature magnetic susceptibility about 100 times larger than that of pure Sr_2RuO_4 [13]. This suggests that the low-lying tilt modes are strongly coupled to the magnetism. This interpretation is further supported by the fact that in all magnetically ordered structures, $x=0.0$, $x=0.1$ and in $\text{O-Ca}_2\text{RuO}_4$, the spin-direction is parallel to the tilt axis in spite of a different octahedron shape as it is schematically drawn in figure 10. Further decrease of the Sr-content below $x=0.5$ stabilizes the tilt and causes a maximum in the temperature dependence of the susceptibility at $T=T_P$,

indicated in Fig. 10 [13]. T_P , however, does not coincide with the structural transition from $\text{I4}_1/\text{acd}$ to the tilted phase but is much lower. We speculate that the susceptibility maximum arises from an increase of anti-ferromagnetic fluctuations induced by the tilt.

There is another anomalous feature in the temperature dependent susceptibility of samples with $0.2 < x < 0.5$: Nakatsuji et al. find a strong anisotropy between the a and b -directions of the orthorhombic lattice [13]. The details of the tilt and rotation distorted structure observed for single crystals in this Sr-range have still to be clarified, but at least for $x=0.2$ the crystal structure is known, see Table I. The complex structure combining the one- c tilt with the two- c rotation should be identical as far as a single layer is concerned. In relation to the magnetic order in the insulating compounds it appears again most likely that the tilt axis, which is parallel b , is the cause of the huge anisotropy. However, there might be an additional more complex effect related to the band structure, which is described for Sr_2RuO_4 for example in reference [10]. Three bands are crossing the Fermi-level: a quasi-two-dimensional band related to the d_{xy} -orbitals and quasi-one-dimensional bands related to d_{xz} - and d_{yz} -orbitals. The elongation of the octahedron basal plane will lift the degeneracy between d_{xz} and d_{yz} -orbitals (in order to demonstrate this, one may choose an orbital set rotated around the c -axis by 45°) and might via this mechanism enhance the anisotropy.

One might also argue that the splitting of the Ru-O(1)-distances which is allowed in L-Pbca is related to a Jahn-Teller effect [14]. However, there is no clear experimental evidence for such a splitting, fits of similar agreement may be obtained when constraining the bonds to equal length (R_{wp} increases in all cases by less than 0.02%). Furthermore, these bonds are not pointing along the direction of the observed anisotropy but along the diagonals of the orthorhombic lattice, and, finally, short and long bonds would be alternating in the sense that a Ru-O-Ru path always consists of a short and a long bond. Hence, even though it is possible that Ru-O(1) distance splitting might be related to orbital ordering, it could not explain the observed magnetic anisotropy.

For Sr concentrations lower than 0.2 we find the Pbca symmetry and the first order phase transition leading to the insulating S-Pbca phase. The metal-insulator transition is hence observed as a function of concentration as well as a function of temperature.

In the Sr range $0.2 \leq x \leq 2$ all samples are found to be metallic at low temperature and there is little variation of the octahedron shape and in particular of the in-plane Ru-O bond lengths when compared to that observed in Sr_2RuO_4 [25, 26]. The concentration dependent octahedron shape is shown in Fig. 12. Metallic 214-ruthenates appear to be identical at least concerning their Ru-O-bond distances. The minor deviation near $x=0.2$ may be explained by the relaxed constraint in the tilted struc-

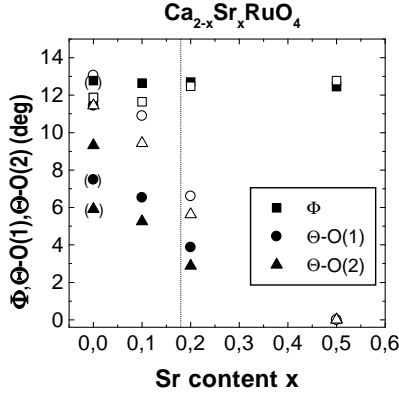


FIG. 11: The Sr concentration dependence of the tilt Θ -O(1) and Θ -O(2) and rotation angle Φ in $\text{Ca}_{2-x}\text{Sr}_x\text{RuO}_4$. The filled symbols denote the results obtained at $T=300$ K (those with brackets are obtained at $T=400$ K) and the open symbols those at $T=10$ K, the dashed line indicates the critical concentration below which one observes the insulating S-Pbca phase at low temperature.

ture. For smaller Sr-content the metal insulator transition occurs, but one may still compare to the Ru-O(1)-bonds in the metallic high temperature phase. For this purpose we have scaled the high resolution results in the metallic phase of the three samples presenting the metal insulator transition, stoichiometric Ca_2RuO_4 , $\text{O-Ca}_2\text{RuO}_4$ and $\text{Ca}_{1.9}\text{Sr}_{0.1}\text{RuO}_4$, by the thermal expansion of Sr_2RuO_4 [26, 27]. Also these values are comparable to pure Sr_2RuO_4 , which demonstrates the equivalence of the metal insulator transition as function of temperature and as function of concentration.

Concerning the metal insulator transition it appears necessary to separate two effects. In all samples exhibiting an insulating low temperature phase there is an increase of the in-plane bond lengths and a reduction of the Ru-O(2)-distance accompanied with the increase of the tilt angle. These effects have to account for the non-metallic behavior. Within a Mott-scenario [16] one may phenomenologically explain the effect, since both tilting and increase of the in-plane distances should strongly reduce the band-width. In particular the band corresponding to the d_{xy} -orbital should become more localized and lower in energy. Assuming that there is a sizeable Hubbard U in these ruthenates, the U/W -ratio might then pass above one explaining the nonmetallic behavior.

In the stoichiometric compound the transition is not complete immediately below T_S ; instead the octahedron becomes flattened mainly due to the elongation of the basal plane along the b-axis which is the direction of the spins in the antiferromagnetic ordered structure. We do not think that this rather peculiar behavior can be explained by simple structural arguments. It appears likely that the spin-orbit coupling in the non-metallic phase causes the low temperature structural anomalies. The

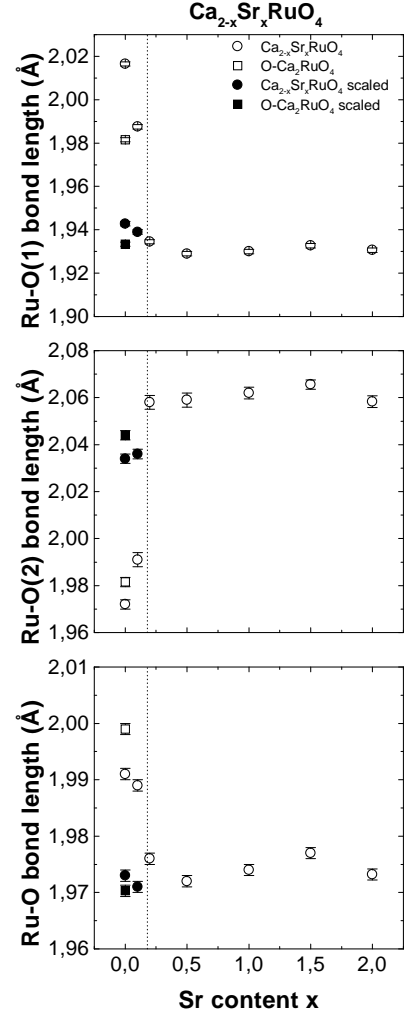


FIG. 12: Composition dependence of the Ru-O(1)-, Ru-O(2)- and averaged Ru-O-bond distances in $\text{Ca}_{2-x}\text{Sr}_x\text{RuO}_4$ at 10 K open symbol. Filled symbols were obtained by extrapolating the distances obtained in the high temperature metallic phase to 10 K using the thermal expansion of Sr_2RuO_4 ; the dashed line designates the critical concentration for the metal insulator transition.

reason why similar effects do not occur in $\text{O-Ca}_2\text{RuO}_4$ and in $\text{Ca}_{1.9}\text{Sr}_{0.1}\text{RuO}_4$ might be found in their remaining itinerant character. Spin-orbit coupling also forces the spin direction parallel to the tilt-axis, which will strongly reduce the weak ferromagnetism along the c-direction. Due to the flattening the d_{xy} -orbital should be well separated in energy and be filled, see also the discussion in [14]. The remaining two electrons occupy the d_{xz} and d_{yz} -orbitals whose degeneration is lifted by the elongation of the octahedron basal plane along b by spin-orbit coupling or by a Jahn-Teller effect [8].

CONCLUSION

The phase diagram of $\text{Ca}_{2-x}\text{Sr}_x\text{RuO}_4$ shows a variety of different structural magnetic and electronic phases. The distinction between metallic and insulating compounds appears to arise from an enhanced in-plane Ru-O bond distance and a larger tilt. This behavior suggests the interpretation as a Mott-transition related to the lowering in energy of the d_{xy} -band. Samples with strongly flattened octahedra are driven non-metallic by the structural transition, whereas in a sample with a reduced flattening the metal-insulator transition is close to the magnetic ordering. The local character of the moments in the insulator induces an additional structural distortion via spin-orbit coupling.

In the part of the phase diagram where samples stay metallic to low temperature, first a rotation and second a tilt distortion develops upon increase of the Ca-content. This should be considered as the purely structural consequence of the smaller ionic radius of the Ca. The observation of the maxima in the temperature dependence of the magnetic susceptibility only for samples presenting an octahedron tilt, and the fact that the maximum low temperature susceptibility is found near the composition where the tilt distortion vanishes, clearly indicate strong magneto-elastic coupling.

The tilt seems to play a key role in the magneto-elastic coupling since in all magnetically ordered structures the spin direction is parallel to the tilt even though the shape of the octahedron is rather distinct. Furthermore, in the intermediate metallic region, $0.2 < x < 0.5$, which exhibits a tilt distortion, a strong anisotropy is found for the susceptibility parallel and perpendicular to the tilt axis. Due to purely structural constraints the tilt leads to an elongation of the octahedron basal plane, which may lift the degeneracy of the d_{xz} and d_{yz} -orbitals.

The magnetic and electronic degrees of freedom in the 214-ruthenates are hence closely coupled to each other and also to the lattice. Whether one of these couplings – and which one – is responsible for the occurrence of superconductivity in Sr_2RuO_4 , however, remains an open question.

We wish to acknowledge D.I. Khomskii, I.I. Mazin and P. Pfeuty for stimulating discussions.

-
- [1] Y. Maeno, H. Hashimoto, K. Yoshida, S. Nishizaki, T. Fujita, J.G. Bednorz, and F. Lichtenberg, *Nature (London)* **372**, 532 (1994).
 - [2] K. Ishida, H. Mukuda, Y. Kitaoka, K. Asayama, Z. Q. Mao, Y. Mori, and Y. Maeno, *Nature (London)* **396**, 658 (1998)
 - [3] J. J. Neumeier, M. F. Hundley, M. G. Smith, J. D. Thompson, C. Allgeier, H. Xie, W. Yelon and J. S. Kim,

- Phys. Rev. B* **50**, 17910 (1994).
- [4] Y. Maeno, K. Yoshida, H. Hashimoto, S. Nishizaki, S. Ikeda, M. Nohara, T. Fujita, A.P. Mackenzie, N.E. Hussey, J.G. Bednorz, and F. Lichtenberg, *J. Phys. Soc. Jpn.* **66**, 1405 (1997).
- [5] T. M. Rice and M. Sigrist, *J. Phys. Cond. Matt.* **7**, L643 (1995).
- [6] A. Callaghan, C. W. Moeller, and R. Ward, *Inorg. Chem.* **5**, 1572 (1966); J. M. Longo, P. M. Raccach, and J. B. Goodenough, *J. Appl. Phys.* **39**, 1372 (1968).
- [7] S. Nakatsuji, S. Ikeda, and Y. Maeno, *J. Phys. Soc. Jpn.* **66**, 1868 (1997).
- [8] M. Braden, G. André, S. Nakatsuji, and Y. Maeno, *Phys. Rev. B* **58**, 847 (1998).
- [9] G. Cao, S. McCall, M. Shephard, J.E. Crow, and R.P. Guertin, *Phys. Rev. B* **56**, R2916 (1997).
- [10] I. I. Mazin and D.J. Singh, *Phys. Rev. Lett* **79**, 733 (1997).
- [11] Y. Sidis, M. Braden, P. Bourges, B. Hennion, S. Nishizaki, Y. Maeno, and Y. Mori, *Phys. Rev. Lett.* **83**, 3320 (1999).
- [12] C. S. Alexander G. Cao, V. Dobrosavljevic, S. McCall, J. E. Crow, E. Lochner, and R. P. Guertin, *Phys. Rev. B* **60**, R8422 (1999); note that the temperature dependence of the lattice constants does not agree to our results.
- [13] S. Nakatsuji, T. Ando, Z. Mao, and Y. Maeno, *Physica C* **259**, 949 (1999); S. Nakatsuji and Y. Maeno, *Phys. Rev. Lett.* **84**, 2666 (2000).
- [14] S. Nakatsuji and Y. Maeno, to appear in *Phys. Rev. B* (2000) September 1st issue.
- [15] G. Cao, S. McCall, C.S. Alexander, J.E. Crow, and R.P. Guertin, *Phys. Rev. B* **61**, R5053 (2000).
- [16] N. F. Mott, *Metal-Insulator Transitions*, 2nd ed. (Taylor & Francis, London, 1990).
- [17] W. Bao, C. Broholm, G. Aeppli, S.A. Carter, P. Dai, T.F. Rosenbaum, J.M. Honig, P. Metcalf and S.F. Trevino, *Phys. Rev. B* **58**, 12727 (1998).
- [18] S. Nakatsuji et al., unpublished.
- [19] M. Braden, P. Schweiss, G. Heger, W. Reichardt, Z. Fisk, K. Gamayunov, I. Tanaka, and H. Kojima, *Physica C* **223**, 396 (1994).
- [20] M. Braden et al., unpublished.
- [21] M. K. Crawford, M. A. Subramanian, R. L. Harlow, J. A. Fernandez-Baca, Z. R. Wang, and D. C. Johnston, *Phys. Rev. B* **49**, 9198 (1994).
- [22] Q. Huang, J. L. Soubeyroux, O. Chmaissem, I. Natali Sora, A. Santoro, R. J. Cava, J. J. Krajewski, and W. F. Peck, Jr., *J. Solid State Chem.* **112**, 355 (1994).
- [23] M. A. Subramanian, M. K. Crawford, R. L. Harlow, T. Ami, J. A. Fernandez-Baca, Z. R. Wang, and D. C. Johnston, *Physica C* **235-240**, 743 (1994).
- [24] M. Braden, W. Reichardt, S. Nishizaki, Y. Mori, and Y. Maeno, *Phys. Rev. B* **57**, 1236 (1998)
- [25] M. Braden, H. Moudden, S. Nishizaki, Y. Maeno, and T. Fujita, *Physica C* **273**, 248 (1997).
- [26] O. Chmaissem, J. D. Jorgensen, H. Shaked, S. Ikeda, and Y. Maeno, *Phys. Rev. B* **57**, 5067 (1998).
- [27] The scaling by the thermal expansion of pure Sr_2RuO_4 is not fully justified, since the temperature dependent tilt and rotation should alter the thermal expansion. This and the insertion of additional oxygen should explain the minor deviations.